

pubs.acs.org/JAFC Article

Stereoselective *In Vitro* Metabolism, Hepatotoxicity, and Cytotoxic Effects of Four Enantiomers of the Fungicide Propiconazole

Siman Ma, Lanfang Ma, Yanbei Lu, Jialin Zhang, Hao Xin, Yuchen Zhou, Shiwen Feng, Ge Jin, Xinyuan Du, Hong Zhang,* and Shiliang Yin*



Cite This: J. Agric. Food Chem. 2024, 72, 27775-27786



ACCESS

III Metrics & More

Article Recommendations

Supporting Information

ABSTRACT: Propiconazole (PRO) is a chiral triazole fungicide that has been widely used for several years. However, its metabolic characteristics and hepatotoxicity in the chiral level environment remain unclear. In this study, the stereoselective behavior of PRO was investigated by using liver microsome incubation, cell viability assay, inhalation exposure, and molecular docking. Our results demonstrated that the isomers trans (–)-2R,4R-PRO and cis (+)-2R,4S-PRO exhibited slower metabolic rates in rat liver microsomes. The cytochrome P450 family 1 subfamily A polypeptide 2 enzyme was found to play a key role in the metabolism of PRO, contributing to its stereoselective behavior. Histopathological and cell viability results showed that exposure to rac-PRO could induce severe hepatotoxicity in mice. This effect might be related to the accumulation of cis (+)-2R,4S-PRO in the liver, which has a slow metabolism and is highly toxic. Our findings indicate that avoiding the application of cis (+)-2R,4S-PRO in agriculture can significantly reduce adverse effects on nontarget organisms.

KEYWORDS: propiconazole, rat liver microsomes, molecular docking, enzyme kinetics, hepatotoxicity

1. INTRODUCTION

In recent years, foodborne pollutants have received widespread attention in environmental research. According to the World Health Organization, approximately 600 million individuals are facing health risks and potential fatalities associated with the consumption of contaminated food. Pesticides are a series of chemical substances that play a significant role in preventing, alleviating, and eliminating plant diseases, insect, and weed growth. The application of pesticides can reduce annual crop yield losses by 30–40%, saving nearly \$300 billion in economic losses globally. However, the off-target effects of excessive agricultural chemical use not only have adverse effects on flora and fauna but also increase the risk to human health. Most chemicals have mammalian toxicity, including carcinogenicity, reproductive toxicity, and thyroid disruption and so on. S

Chiral pesticides had occupied an increasingly large proportion of the global pesticide market. Owing to their chiral structures, the enantiomers of these pesticides exhibit distinct characteristics in absorption, biodegradation, and metabolism within chiral environments. After inevitably lingering on target organisms (e.g., vegetables, fruits, and creeps) and soil surfaces during application,8 these chiral pesticides are introduced into the organisms through multiple exposure routes, including oral intake, skin contact, and respiratory inhalation. As the most significant metabolic organ, the liver contains a diverse array of metabolic enzymes such as the phase I metabolic enzyme family known as cytochromes P450 (CYPs). These enzymes facilitate the oxidation, reduction, and hydrolysis of chiral pesticides in the liver. This process creates a chiral environment in vivo, leading to stereoselective metabolism and higher accumulation of one toxic isomer or its metabolites. 10-13 This leads to hepatotoxicity and liver dysfunction, including hepatic enzyme abnormality, necrosis of hepatocellular, jaundice, and acute liver failure. 14 Many studies using an in vitro liver microsome incubation system, which eliminates interference from internal factors, 15 corroborated these results. For example, the half-life of S-uniconazole (74.5 min) in rat liver microsomes (RLMs) was nearly two times higher than that of the R-enantiomer (38.7 min). Additionally, R-uniconazole showed stronger binding to cytochrome CYP2D2.¹⁶ A study on the oxidative metabolism of prothioconazole-desthio by human liver microsomes has demonstrated that the (+)-isomer was preferentially metabolized. ¹⁷ Additionally, (-)-1*S-cis-\alpha R*-cypermethrin had a faster metabolic rate in RLMs than (+)-1R-cis-αS-cypermethrin.¹⁸ Although many studies have reported the hepatotoxicity of chiral pesticides, these studies focused on only their racemates. For example, cypermethrin exposure could affect the proteasome pathway in grass carp liver cells (L8824) and cause intoxication.¹⁹ Moreover, the exposure of mice to racprothioconazole and its metabolite could induce severe hepatic metabolism disorder and oxidative stress, and its metabolite caused more severe adverse effects than its parent compound.²⁰ The differences in metabolism of these chiral pesticides in the liver and the hepatotoxicity of their enantiomers remain unclear.

Received: July 31, 2024 Revised: November 29, 2024 Accepted: December 2, 2024

Published: December 10, 2024





Figure 1. Chemical structures of PRO enantiomers ((a) cis (+)-2R,4S-PRO; (b) cis (-)-2S,4R-PRO; (c) trans (-)-2R,4R-PRO; d, trans (+)-2S,4S-PRO).

PRO (Figure 1) is a triazole fungicide that possesses two chiral centers and four enantiomers. PRO inhibits lanosterol- 14α -demethylase, blocking fungal cell membrane synthesis and treating diseases such as Alternaria black spot, anthracnose, gray mold, and powdery mildew in fruits, vegetables, and crops.^{21–24} The bioactivity sequence of PRO enantiomers against the pathogen Magnaporthe oryzae was 2R,4S > 2S,4R > Rac > 2R,4R > 2S,4S; for the pathogen *Ustilaginoidea virens*, the sequence was 2R,4S > 2S,4R > 2R,4R > Rac > 2S,4S; and for the pathogen Fusarium moniliforme, the sequence was 2R,4S >Rac > 2S,4R > 2S,4S > 2R,4R. However, for the *Thanatephorus* cucumeris and Rhizoctonia solani pathogens, the bioactivity of trans PRO isomers is stronger than that of cis-PRO. 25 Exposure to isomers of PRO or rac-PRO could lead to severe liver toxicity in mice and rats. 26,27 The studies on the underlying mechanism revealed that the hepatotoxicity of PRO was related to oxidative damage to cellular proteins, 28 liver fibrosis, ²⁹ the increase of mRNA expression and enzyme activity of CYP1A1 and CYP1A2,30 and hepatocyte hypertrophy.² However, these studies have mainly focused on the racemate of PRO. In our previous tissue distribution study in a chiral environment, we found that PRO had the highest accumulation levels in the liver, and its four isomers showed distribution characteristics in the liver related to their stereochemistry.³¹ Therefore, investigating the relative metabolic rates and the main CYP metabolic enzyme of PRO enantiomers in a chiral environment could help further elucidate the causes and mechanisms of PRO hepatotoxicity.

In the current study, we first established an *in vitro* incubation system using RLMs to investigate the stereoselective metabolic characteristics of PRO enantiomers using the chiral liquid chromatography with the tandem mass spectrometry (LC–MS/MS) method based on our previous study.³¹ Subsequently, an enzyme kinetic assay was conducted to evaluate the intrinsic clearance capacity of the PRO isomers

in RLMs. Moreover, to elucidate the possible mechanisms underlying the stereoselective metabolic differences, a molecular docking technique was employed to establish homologous models using the five CYP450 proteins and each PRO isomer. Subsequently, the hepatotoxicity resulting from inhalation exposure to PRO in mice was investigated to indirectly evaluate the potential risks to the agricultural special working groups in vivo. Based on the hepatotoxic results, we used a 3-(4,5-dimethylthiazol-2-yl)-2,5-diphenyltetrazolium bromide (MTT) assay to identify the most toxic PRO isomer at the chiral level causing hepatotoxicity. We innovatively studied the stereoselective metabolic characteristics of PRO enantiomers in the RLM system and evaluated the potential hepatotoxicity of PRO exposure at in vivo and in vitro levels. This study identifies the safest single enantiomer of PRO to prevent the toxic effects of rac-PRO on nontarget organisms. Additionally, the findings may inspire further research on reducing the potential adverse effects of chiral pesticides on nontarget organisms.

2. MATERIALS AND METHODS

2.1. Reagents. The *rac*-PRO with a purity higher than 98.0% and isomer ratio of 2.11:2.11:2.89:2.89 (determined using Chiralpak IG) was purchased from Aladdin (Shanghai, China). The optical isomers of PRO with a purity higher than 99.0% were experimentally enantioseparated by Daicel (Shanghai, China). The internal standard (IS) of doxylamine was obtained from Aladdin. The MS-grade acetonitrile was purchased from Fisher Scientific (Fair Lawn, NJ, USA). The ultrapure water was obtained using a MUL-9000 water purification system (Nanjing Zongxin Water Equipment Co., Ltd., China). The standard stock solutions of *rac*-PRO and IS (1.0 mM/L) used for *in vitro* RLM incubation were dissolved in acetonitrile and stored at 4 °C. β -Nicotinamide adenine dinucleotide phosphate (NADPH) was purchased from Solarbio (Shanghai, China). The phosphate-buffered saline (PBS) solution was procured from Haoyuan (Shanghai, China). The MTT solution was obtained from

Sigma-Aldrich (St. Louis, MO, USA). The ethanol solutions of *rac*-PRO, *trans* (-)-2*R*,4*R*-PRO, *trans* (+)-2*S*,4*S*-PRO, *cis* (+)-2*R*,4*S*-PRO, and *cis* (-)-2*S*,4*R*-PRO (100 mM/L) were stored protected from light at 4 °C. The L02 cell line (human embryonic liver cells) and HepG2 cell line (hepatoma cells) were purchased from the American Type Culture Collection (Manassas, VA, USA). Fetal bovine serum and Dulbecco's modified Eagle medium were obtained from Gibco (Grand Island, NY, USA).

- **2.2. Animals.** Sprague—Dawley rats (180–220 g) and Kingming (KM) mice (18–22 g) were provided by Huafukang (Beijing, China). The animals were housed in the specific pathogen-free laboratory with the environmental conditions of 22 °C \pm 2 °C and 12 h of alternation of light and dark. All of the animals were free to consume food and water. Our research complied with the principles of the Helsinki Declaration and was approved by the Institutional Animal Care and Use Committee of Shenyang Pharmaceutical University (SYPU-IACUC-S2023-1227-110).
- **2.3. Preparation of RLMs.** After euthanizing the male Sprague—Dawley rats (180–220 g) used for RLM preparation, we dissected their livers on ice as soon as possible. Subsequently, we weighed and homogenized the liver tissue in an ice-cold PBS buffer (w/v, 1:10). After centrifuging the samples for 15 min (3,000 × g, 4 °C), the obtained supernatant was collected and centrifuged for another 30 min (12,000 × g, 4 °C). Subsequently, we continued to aspirate and centrifuge the supernatant for 1 h (105,000 × g, 4 °C). Subsequently, we added PBS to resuspend the liver microsomal precipitate and diluted it to 4.0 mg/mL. After using the BCA Protein Quantification Kit (Thermofisher, USA) to determine the protein concentrations of RLM samples, the obtained RLM samples were stored at -80 °C before incubation.
- 2.4. Metabolism of PRO Enantiomers in RLMs. We used the substrate depletion experiments, which were conducted in the in vitro RLM incubation system, to investigate the stereoselective metabolic characteristics of the PRO enantiomers over time. Briefly, we prepared a mixed reaction system of 400 μ L, which included PBS buffer (pH = 7.4), NADPH (dissolved in PBS solution, 1.0 mM/L), MgCl₂ (2.0 mM/L), RLMs (1.0 mg/mL protein concentration), and the target compounds with a final concentration of 150 µmol/L rac-PRO (dissolved in acetonitrile). The proportion of acetonitrile in the RLM should be less than 1.0% (ν/ν) . The RLM incubation system was preincubated at 37 °C for 5 min. Subsequently, an NADPH solution of 1.0 mM/L was added to activate the reaction. After incubating the system for 0-120 min (0, 5, 15, 30, 45, 60, 90, and 120 min) in a concussion water bath at 37 °C, we added 1.0 mL of precooled acetonitrile and vortexed the mixture for 1 min to stop the reaction. After the mixture was centrifuged at $12,000 \times g$ for 10 min and filtered, 10 μ L of the sample was analyzed using the LC-MS/MS system. The control group without NADPH was performed in triplicate. The metabolism of PRO isomers over time in the in vitro incubation system followed the first-order kinetic eq 1.32 Subsequently, the $t_{1/2}$ values of each stereoisomer were evaluated with eq 2.33 Moreover, we used eq 3 to calculate the enantiomeric fractions $(EF)^{16}$

$$C_t = C_0 e^{-kt} \tag{1}$$

$$t_{1/2} = \ln 2/k = 0.693/k \tag{2}$$

$$EF_{trans} = C_{2R,4R} / (C_{2R,4R} + C_{2S,4S}) \text{ and } EF_{cis}$$

$$= C_{2R,4S} / (C_{2R,4S} + C_{2S,4R})$$
(3)

where C_0 represents the concentration (μ mol/L) at time 0 (min), and C_t represents the concentration (μ mol/L) at time t (min). The value of k represented the rate constant of the metabolism reaction, and the value of $t_{1/2}$ represented the half-life time (min). The $C_{(isomer)}$ was the concentration of each specified enantiomer. The EF_{tran} and EF_{cis} represented the EF of *trans*- and *cis*-PRO, respectively.

2.5. Enzyme Kinetic Assay of PRO Enantiomers. In the present study, a series of concentrations of each PRO isomer ranging from 5.0 to 250.0 μ mol/L were constructed according to the above-

mentioned incubation system for the enzyme kinetic test. The incubation procedures were the same as those in Section 2.4, with the incubation time set to 30 min. Subsequently, vital parameters of PRO enantiomers were obtained by using the Michaelis—Menten equation. The values of V and $K_{\rm m}$ were calculated with eq 4, 34 and the ${\rm CL}_{\rm int}$ was evaluated with eq 5. 35

$$V = V_{\text{max}} \times S / (K_{\text{m}} + S) \tag{4}$$

$$CL_{int} = V_{max}/K_{m}$$
 (5)

The parameters of V, $V_{\rm max}$, S, $K_{\rm m}$, and $CL_{\rm int}$ represent the metabolism rate, maximum metabolism velocity, substrate concentration, Michaelis constant, and intrinsic metabolic clearance, respectively. The nonlinear regression curves of substrate concentration versus reaction velocity were simulated using the Michaelis—Menten equation in Origin 8.0 software.

- 2.6. Molecular Docking Study. Herein, homology modeling and molecular docking were used to elucidate the reasons why different PRO isomers exhibited different metabolic rates in the RLMs. The P450 enzymes are the most significant enzyme system and are responsible for the metabolism of exogenous and endogenous chemicals. Therefore, according to the crystal structures of human liver microsomes, we selected five major P450 enzymes in the liver (CYP1A2, CYP2C11, CYP2E1, CYP3A1, and CYP2D6) to investigate the interactions between PRO isomers and enzymes. The crystal structures of human CYP1A2 (PDB ID: 2HI4), CYP2C11 (PDB ID: 1R9O), CYP2D6 (PDB ID: 4WNV), CYP2E1 (PDB ID: 3E4E), and CYP3A1 (PDB ID: 4NY4) were obtained from the protein data bank (http://www.rcsb.org/pdb/home/home.do). For CYP homology modeling, the Modeler 9.11 software was used to construct the crystal structures of rats based on sequence alignment. We used Prime software to optimize the constructed crystal structures before molecular docking. Thereafter, the AutoDock software originated from the MGL Tools 1.5.6 package and was selected to conduct molecular docking between each PRO isomer and target CYP enzyme. The figures of these ligand sites were acquired from PyMol (DeLano Scientific, Palo Alto, CA, USA). The binding energy between the PRO isomer and the subjected receptor was calculated, and the software package Gaussian 09W was used to minimize the energy. Subsequently, the PRO isomers were docked to the CYP binding sites separately, and the conformer with the lowest energy was selected as the most likely bioactive conformer.3
- **2.7. Toxicological study.** We randomly divided the 40 KM mice (half male and half female) into four groups: the control group and three *rac*-PRO exposure groups (121.5, 243.0, and 486.0 mg/kg). We placed the mice into the atomization instrument, which includes an atomizer and a sealed box to inhale *rac*-PRO, to simulate the peasant's exposure to PRO during the process of agricultural spray. The inhalation dosages of *rac*-PRO were calculated according to the median lethal dose of rat inhalation exposure (5,800 mg/m³/4 h), mouse and rat dosage conversion coefficient, and sealed atomizing box volume. After inhalation with *rac*-PRO for 14 days, blood was collected through the retinal venous plexus. Subsequently, the mice were euthanized, and the livers of the mice were dissected for further studies.
- **2.8.** Histopathological Examination. After fixing it with a 10% formalin solution for 24 h, the liver tissue was dehydrated using an automatic tissue processor (Taikang, China). Subsequently, the tissue was embedded into the paraffin and was sectioned into 4 μ m-thick sections using the semiautomatic rotary microtome (Leica, Germany). We stretched out to prepare these sections on histological slides and dried them overnight. After staining sections with the hematoxylin–eosin stain, we observed the pathohistological changes of liver cells using the Nikon DS-Ri2 light microscope (Nikon, Japan) under 200× magnification.
- 2.9. Enzyme-Linked Immunosorbent Assay Assessment of the Biochemistry Indexes. The levels of glutamic-pyruvic transaminase, glutamic oxaloacetic transaminase, uric acid, and total bile acid in the serum of mice were examined using the enzyme-linked immunosorbent assay kit (MEIMIAN Co., Ltd., China). Briefly, after

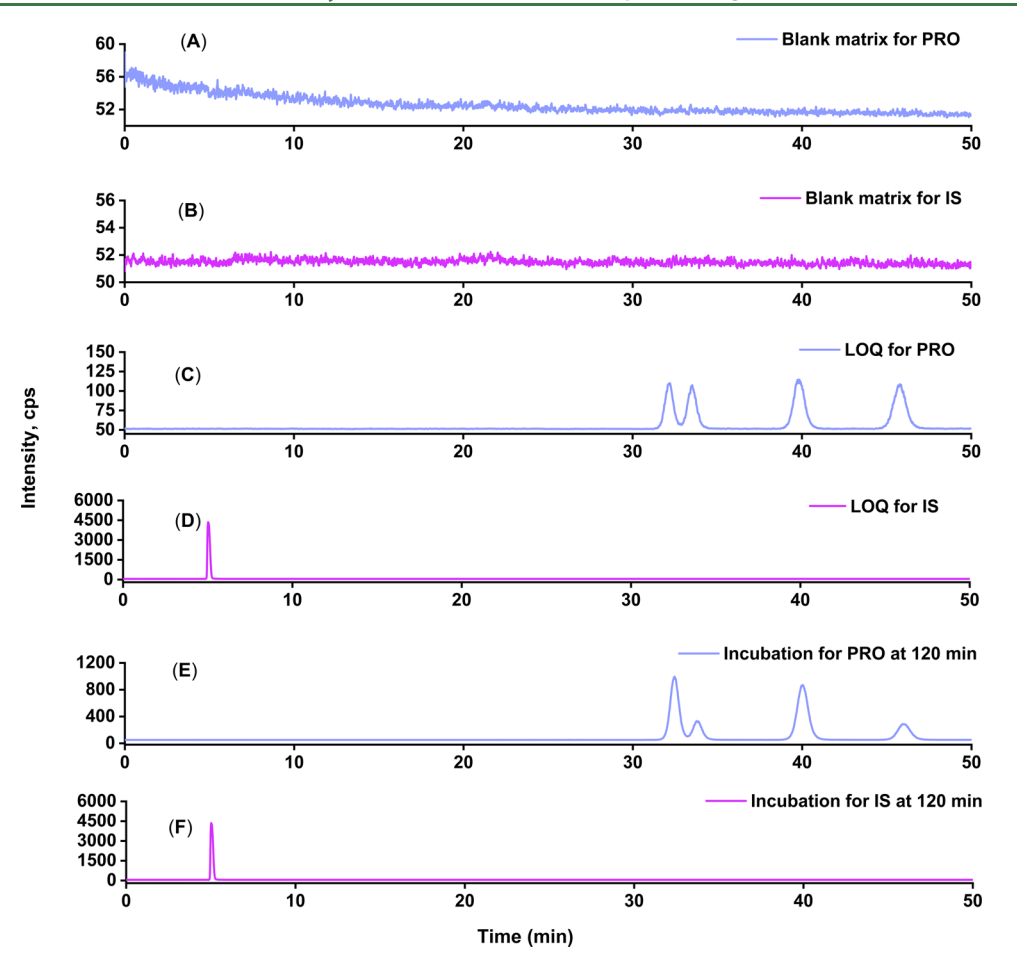


Figure 2. Representative chromatograms of PRO enantiomers and IS in blank RLM samples (A&B), blank RLM samples spiked at LLOQ level of 0.05 μ mol/L rac-PRO (C&D), and actual RLM samples and IS with the incubated concentration of 150 μ mol/L at 120 min (E&F).

Table 1. Precision and Accuracy for the Developed Chiral LC-MS/MS Method in RLM Matrix

		1					
		intraday(n = 6)		interday(n = 18)			
analytes	nominal concentration $(\mu M/L)$	calculated concentration $(\mu \mathrm{M/L})$	RE (%)	RSD (%)	calculated concentration $(\mu \mathrm{M/L})$	RE (%)	RSD (%)
trans (-)-2R,4R-PRO	0.011	0.010 ± 0.001	-9.1	10.0	0.010 ± 0.001	-9.1	10.0
	0.84	0.90 ± 0.06	7.1	6.7	0.91 ± 0.08	8.3	8.8
	8.4	8.9 ± 0.4	6.0	4.5	9.0 ± 0.5	7.1	5.5
	16.9	15.9 ± 0.9	-5.9	5.7	16.1 ± 0.8	-4.7	5.0
trans (+)-2S,4S-PRO	0.011	0.010 ± 0.001	-9.1	10.0	0.010 ± 0.001	-9.1	10.0
	0.84	0.90 ± 0.06	7.1	6.7	0.91 ± 0.08	8.3	8.8
	8.4	8.8 ± 0.5	4.8	5.7	9.0 ± 0.6	7.1	6.7
	16.9	15.9 ± 0.9	-5.9	5.7	16.1 ± 0.7	-4.7	4.3
cis (+)-2R,4S-PRO	0.014	0.013 ± 0.001	-7.1	7.7	0.013 ± 0.001	-7.1	7.7
	1.16	1.20 ± 0.07	3.4	5.8	1.24 ± 0.06	6.9	4.8
	11.6	11.9 ± 0.8	2.6	6.7	11.9 ± 0.6	2.6	5.0
	23.1	21.9 ± 1.4	-5.2	6.4	22.7 ± 0.9	-1.7	4.0
cis (-)-2S,4R-PRO	0.014	0.0130 ± 0.001	-7.1	7.7	0.013 ± 0.001	-7.1	7.7
	1.16	1.21 ± 0.07	4.3	5.8	1.23 ± 0.05	6.0	4.1
	11.6	12.1 ± 0.8	4.3	6.6	11.9 ± 0.6	2.6	5.0
	23.1	21.6 ± 1.3	-6.5	6.0	22.4 ± 0.8	-3.0	3.6

10 μ L of the blood serum was added to 40 μ L of the sample diluent, the mixture was placed in a 96-well plate and gently vortexed for 1 min. Subsequently, the mixture was incubated with 100 μ L of horseradish peroxidase-conjugated reagent at 37 °C for 60 min. After aspiration and discarding of the supernatant, the plate was air-dried naturally. Subsequently, we washed the plate five times and air-dried it, and the chromogen solution was added to the plate and incubated

in the dark for 15 min. Finally, the stock solution was added to stop the reaction, and a microplate reader (Biorad, USA) was used to determine the absorbance of the reaction mixture at 492 nm.

2.10. Cell Culture. The Dulbecco's modified Eagle medium was used to incubate the hepatoma cell line HepG2, rat primary hepatocytes, and human embryonic liver L02 cell line. Moreover, 10% heat-inactivated fetal bovine serum, 1% penicillin/streptomycin,

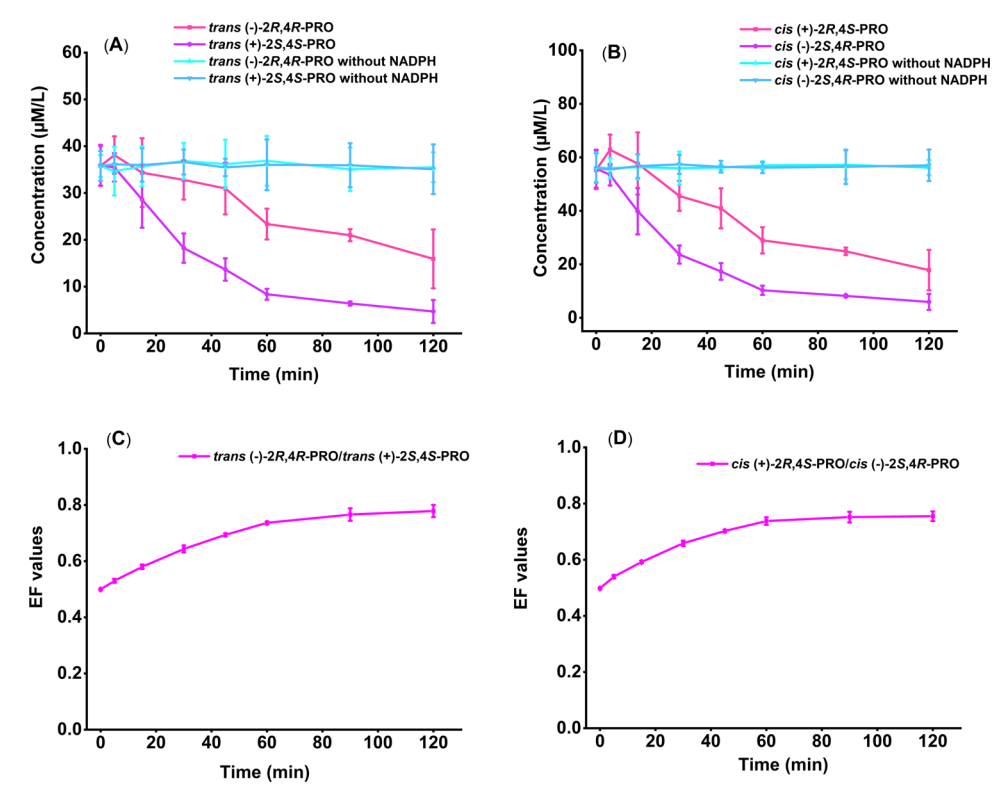


Figure 3. Substrate concentrations of PRO enantiomers in the RLM incubation system (A,B) and the corresponding EF values (C,D).

and 1 mmol/L L-glutamine were added to the culture medium to maintain the *in vitro* culture. Cells were seeded in the 60 cm 2 culture dishes and cultured in the incubator, which was filled with 5% CO $_2$ and the temperature was set at 37 $^{\circ}$ C in a humidified condition.

2.11. Cytotoxicity Examination. The cell viability was determined by using the modified MTT assay to evaluate the cytotoxic effects of rac-PRO and its four enantiomers. Briefly, the cells that were in the logarithmic growth phase were adjusted to a density of 8.0×10^4 cells/mL, seeded on 96-well plates, and incubated for 24 h. Subsequently, the cells were incubated with vehicle (0.1% ethanol) or different concentrations of rac-PRO, trans (-)-2R,4R-PRO, trans (+)-2S,4S-PRO, cis (+)-2R,4S-PRO, and cis (-)-2S,4R-PRO (0.01, 0.05, 0.1, 0.2, and 0.5 mmol/L) for 72 h. To examine the cytotoxic effect of celecoxib, the cells were incubated with different concentrations of celecoxib (10, 20, 50, and 100 µmol/L) for 72 h. Subsequently, the MTT solution (2.5 mg/mL, 10 μ L) was added to each well and incubated for 3-4 h. The culture medium was aspirated, and the resulting solution was discarded. Subsequently, 100 μL of dimethyl sulfoxide was added to each well, and the well was gently vibrated for 10 min. The microplate reader (Biorad) was used to determine the absorbance of the reaction mixture at 492 nm.

2.12. Combination Cytotoxic Effect of PRO Enantiomers and Celecoxib. To further certify the role of the CYP1A2 enzyme in the metabolism of PRO, we used celecoxib, the inhibitor of the CYP1A2 enzyme, to examine whether the inhibition effect of celecoxib CYP1A2 could lead to the metabolic disorder of PRO, resulting in an accumulation of PRO in cells. This increased the cytotoxicity of PRO on the human hepatic L02 cell line. Therefore, we used the MTT assay to examine the synergistic effect of celecoxib and PRO. Briefly, the cells that were in the logarithmic growth phase were adjusted to the density of 8.0×10^4 cells/mL, seeded on the 96-well plates, and incubated for 24 h. After different concentrations of celecoxib (10, 20, 50, and $100~\mu$ mol/L) were added and incubated for 24 h, $100~\mu$ mol/L of the enantiomer of PRO was added and incubated for 48 h. Subsequently, we used the MTT assay to examine the cell viability.

2.13. Data Analysis. All data are expressed as the mean \pm standard error. Subsequently, a one-way analysis of variance followed

by Dunnett's t;test (SPSS 22.0, USA) was used to compare the significant differences between groups. The probability value of p < 0.05 was significant.

3. RESULTS AND DISCUSSION

3.1. Chiral Separation and Method Validation. We separated the enantiomers of PRO based on our previously

Table 2. First-Order Kinetic Constants (k), Half-Lives $(t_{1/2})$, and Correlation Coefficients (R^2) of PRO Enantiomers in the *In Vitro* RLM Incubation System (n = 3)

enantiomers	$k \left(\min^{-1} \right)$	$t_{1/2}$ (min)	R^2	
trans (-)-2R,4R-PRO	0.0119 ± 0.0005	58.24 ± 2.22	0.9469	
trans (+)-2S,4S-PRO	0.0207 ± 0.0010	33.48 ± 1.60	0.9840	
cis (+)-2R,4S-PRO	0.0151 ± 0.0011	45.89 ± 3.19	0.9709	
cis (-)-2S,4R-PRO	0.0222 ± 0.0013	31.22 ± 1.72	0.9733	

Table 3. Metabolic Kinetic Parameters of PRO Enantiomers in the *In Vitro* RLM Incubation (n = 3)

enantiomers	$V_{ m max}~(\mu{ m M} \ { m mgprotein}^{-1} \ { m min}^{-1})$	$K_{\rm m}~(\mu{ m M})$	CL_{int} (mL mgprotein ⁻¹ min ⁻¹)	R^2
trans (-)-2R,4R- PRO	1.53 ± 0.31	80.61 ± 21.83	18.98	0.9507
trans (+)-2S,4S- PRO	3.55 ± 1.06	154.00 ± 32.3	23.05	0.9763
cis (+)-2R,4S- PRO	1.87 ± 0.46	98.57 ± 29.11	18.97	0.9228
cis (-)-2S,4R- PRO	4.51 ± 1.19	172.39 ± 28.96	26.16	0.8559

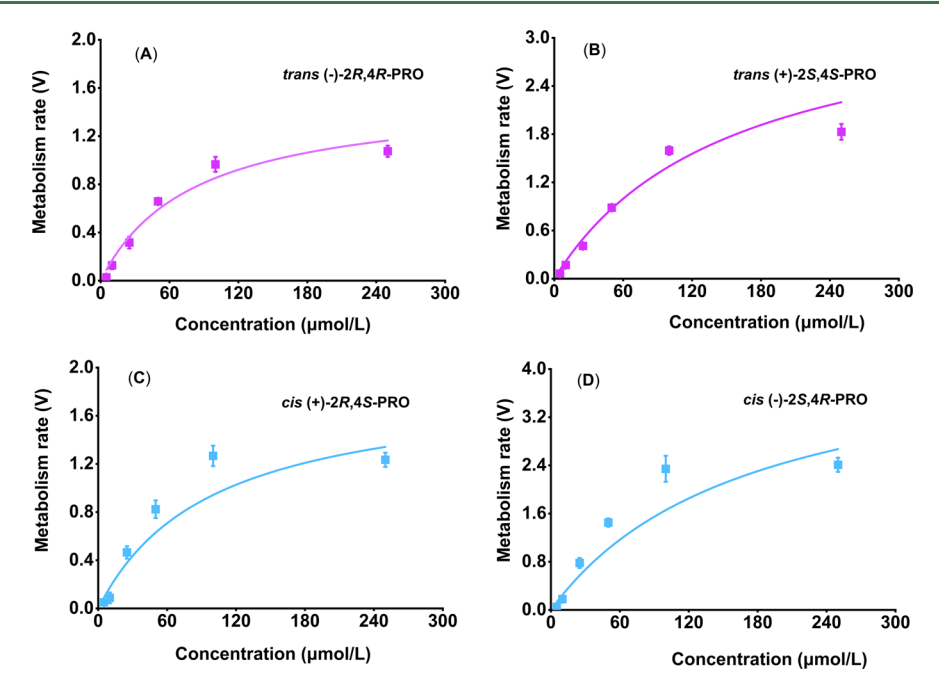


Figure 4. Michaelis-Menten kinetic assay of PRO enantiomers in the in vitro RLM incubation.

established chiral LC-MS/MS method. The typical chromatograms are shown in Figure 2. Additionally, we fully validated the chiral separation method using LC-MS/MS to determine the concentrations of PRO enantiomers in the RLM matrix to ensure its precision and accuracy. There are no endogenous interference peaks around the retention time of PRO enantiomers and IS in the blank RLM samples, which indicates its excellent specificity (Figure 2). The matrix standard curves for rac-PRO with a concentration ranging of 2.5 to 100.0 µmol/L were established by adding a series of working solutions to boiled RLMs blank samples, and greater linearity with R^2 higher than 0.99 was observed (Tables S1 and S2). The lower limit of quantitation of rac-PRO in RLMs was 0.05 µmol/L. The accuracy and precision of the developed method at three QC levels were validated, and the results are shown in Table 1. All these results suggested that our developed method for determining PRO enantiomers was accurate and reprodu-

3.2. Stereoselective Metabolism of PRO Enantiomers in RLMs. NADPH is a significant coenzyme for CYP 450 monooxygenases. Therefore, in the current study, we used the RLM in vitro incubation system with or without NADPH to evaluate the stereoselective metabolism of the PRO enantiomers. The results (Figure 3 and Table 2) indicated that the addition of NADPH could activate the metabolism of PRO enantiomers, but the substrate concentration of the inactivated group did not decrease, which indicated that the energy provided by NADPH was required in the metabolic process of PRO enantiomers. As shown in Figure 3A,B, the results revealed the metabolic curves of trans (-)-2R,4R-PRO, trans (+)-2S,4S-PRO, cis (+)-2R,4S-PRO, and cis (-)-2S,4R-PRO from time 0 to 120 min at the substrate concentration of 150 μ mol/L. Our results indicated that the substrate concentrations of trans (-)-2R,4R-PRO and cis (+)-2R,4S-PRO were 0.99-3.91 and 0.99-3.41 times higher than those of the other two isomers, respectively. This could lead to the relative accumulation of trans (-)-2R,4R-PRO, and cis (+)-2R,4S-PRO in the liver and cause potential hepatotoxicity.

This finding was completely consistent with our previous conclusion that the tissue distribution concentrations of trans (-)-2R,4R-PRO and cis (+)-2R,4S-PRO in the mouse liver were higher than those of trans (+)-2S,4S-PRO and cis (-)-2S,4R-PRO.³¹ Therefore, further investigation and comparison of whether different PRO isomers can induce different hepatotoxic effects are of great significance. Moreover, the data in Table 1 proved that the metabolic rate of each isomer in RLMs followed the first-order kinetics with R^2 higher than 0.9469. Significant differences of half-lives (p < 0.05) were found between trans (-)-2R,4R-PRO and trans (+)-2S,4S-PRO and between cis(+)-2R,4S-PRO and cis(-)-2S,4R-PRO. The $t_{1/2}$ values of trans-PRO and cis-PRO ranged from 33.48 to 58.24 min and from 31.22 to 45.89 min, respectively. The EF values of the trans- and cis-forms gradually increased from 0.50 to 0.80 (Figure 3C,D), which indicated that the PRO enantiomers showed stereoselective metabolism characteristics in RLMs. The literature has shown that the phase I enzymes of the CYP family were related to the metabolisms of endogenous and exogenous chemicals. Therefore, CYP2E1, CYP3A4, and CYP1A2, as the main enzymes of CYPs, might be associated with the stereoselective metabolism of PRO enantiomers owing to the enantiospecific binding effects of PRO isomers to the spatial configuration of chiral proteins. 36,37 Therefore, molecular docking techniques should be used to further explore and elucidate the detailed stereoselective metabolic mechanism of rac-PRO in the RLM incubation system.

3.3. Stereoselective Enzyme Kinetic Assay of PRO Enantiomers in RLMs. To evaluate the enantioselective metabolic characteristics of PRO in RLMs, a substrate consumption experiment was designed to reveal the metabolic kinetics. The representative kinetic parameters of PRO enantiomers, including $V_{\rm max}$, $K_{\rm m}$, R^2 , and ${\rm CL_{int}}$ are summarized in Table 3. In Figure 4A–D, the regression profiles of metabolic reaction rate versus substrate concentration of each isomer were exhibited. For *trans*-forms, the $V_{\rm max}$ and ${\rm CL_{int}}$ of *trans* (+)-2S,4S-PRO were 2.32 and 1.21 times higher than those of *trans* (–)-2R,4R-PRO, respectively, which indicated

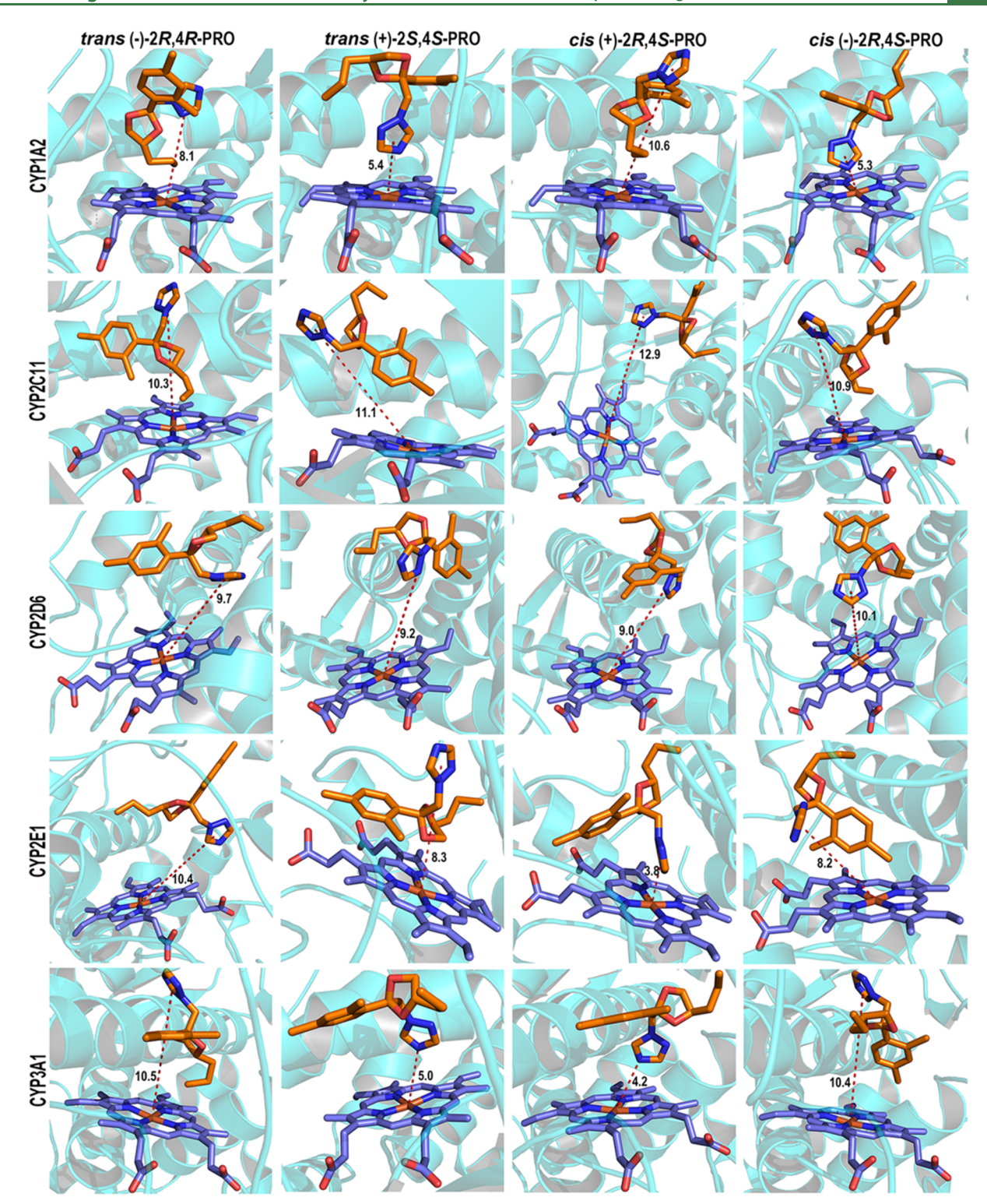


Figure 5. Stereoisomer-specific binding modes of PRO enantiomers with CYP1A2, CYP2C11, CYP2E1, CYP3A1, and CYP2D6 enzymes.

that the metabolic rate and elimination capability of isomer trans (+)-2S,4S-PRO were faster. Moreover, the $K_{\rm m}$ of trans (+)-2S,4S-PRO was 1.91-fold higher than that of its opposite enantiomer. Additionally, the higher $K_{\rm m}$ value and the stronger affinity between chiral compounds and proteins may lead to prior metabolism. The cis-form values of $V_{\rm max}$, $CL_{\rm int}$, and $K_{\rm m}$ of cis (-)-2S,4R-PRO were 2.41, 1.38, and 1.75 times higher than those of cis (+)-2R,4S-PRO, respectively. These results suggested that the isomers of trans (-)-2R,4R-PRO and cis

(+)-2R,4S-PRO represent potential risks to human health and environmental ecology, owing to their slower metabolic rates.

3.4. Molecular Docking between CYP Enzymes and PRO Enantiomers. CytochromeP450 enzymes, as a category of monooxygenase that can catalyze the metabolism of chemicals, mainly exist in the endoplasmic reticulum of the liver and intestinal cells. The P450 enzymes could oxidize exogenous substances by transferring electrons from iron ions in the heme, thereby improving their water solubility.³²

Table 4. Binding Energy of PRO Enantiomers with P450 Enzymes

binding energy (kcal/mol)						
enantiomers	CYP1A2	CYP2C11	CYP2D6	CYP2E1	CYP3A1	
trans (-)-2R,4R- PRO	-7.6	-5.8	-6.4	-6.4	-8.1	
trans (+)-2S,4S- PRO	-8.0	-5.2	-6.2	-6.8	-8.3	
cis (+)-2R,4S-PRO	-6.8	-6.0	-6.2	-8.4	-7.0	
cis (-)-2S,4R-PRO	-7.2	-6.2	-6.0	-7.0	-6.8	

However, the "6 Å rule" was commonly followed, which means that if the binding distance between each isomer and heme Fe is within 6 Å, the P450 enzymes could be effectively responsible for drug metabolism.^{38,39} In Figure 5, the detailed binding distances are shown between the N-atom in the triazole ring of PRO and the Fe ion in five typical P450 enzymes. We calculated the binding energies of four PRO isomers with the targeted P450 enzymes, as shown in Table 4. In the metabolism of CYP2C11 and CYP2D6, the binding distances between the N-atom and the heme Fe were longer than 6 Å, suggesting that the isomers of PRO were not mainly metabolized by them. For the trans-form, the binding distance and energy of trans (+)-2S,4S-PRO with CYP1A2 and CYP3A1 enzymes were shorter and weaker than those of trans (-)-2R,4R-PRO. Our results showed that the binding distances and energies of trans (-)-2R,4R-PRO and trans (+)-2S,4S-PRO with CYP1A2 were 8 and 5.4 Å and -7.6 and -8.0 kcal/mol, respectively. With CYP3A1, the distances and energies of trans (-)-2R,4R-PRO and trans (+)-2S,4S-PRO were 10.5 and 5.0 Å and -8.1 and -8.3 kcal/mol, respectively. Our results indicated that the metabolism of trans (+)-2S,4S-PRO by CYP1A2 and CYP3A1 could be easier than that for trans (-)-2R,4R-PRO, which was completely consistent with our results of the RLM in vitro incubation. For cis-isomers, the faster metabolic rate of cis(-)-2S,4R-PRO was observed in the metabolism by CYP1A2. Therefore, in combination with the in

vitro and in vivo results, the CYP1A2 enzyme was considered the main metabolic enzyme of PRO.

3.5. Inhibitor of the CYP1A2 Enzyme Could Intensify the Cytotoxic Effect of PRO. To confirm the key role of the CYP1A2 enzyme in the metabolism of PRO, celecoxib, the inhibitor of the CYP1A2 enzyme, 40 was used to examine whether inhibition of the CYP1A2 enzyme could lead to an accumulation of PRO in the hepatic cells, resulting in synergistic cytotoxic effects on the hepatic cells. Therefore, we first used the MTT assay to examine the cytotoxicity of celecoxib (Figure 6A). Subsequently, at the concentrations of celecoxib that do not affect the cell viability, we examined the synergistic effect of celecoxib on the cytotoxicity of cis (+)-2R,4S-PRO, which is the most toxic enantiomer of PRO, in human hepatic cell line L02. As shown in our results, although 100 μ mol/L celecoxib could not affect the viability of L02 cells (Figure 8A), different concentrations of celecoxib exacerbated the cytotoxicity of cis (+)-2R,4S-PRO to L02 cells in a concentration-dependent manner (Figure 6B). This result certified that the CYP1A2 enzyme might play a key role in the metabolism of PRO in hepatic cells.

3.6. Hepatotoxicity of PRO. In our previous study, we found that the liver accumulated the highest concentration of PRO among the organs of the mice (the brain, heart, liver, lung, and kidney) and PRO showed stereoselective cytotoxic effects on the neuronal and pulmonary cells. Therefore, it is essential to investigate whether inhalation exposure to PRO could lead to hepatotoxicity and affect the biological functions of the liver in mice. To simulate peasant's exposure to PRO during agricultural spray, inhalation exposure of mice to rac-PRO was conducted to investigate the hepatotoxicity of PRO owing to the limited amount of pure PRO enantiomers obtained. Results in Figure 7A-D reveal that the inhalation administration of rac-PRO for 14 days significantly increased glutamic oxaloacetic transaminase and uric acid levels in mice serum. Moreover, rac-PRO inhalation exposure significantly decreased the total bile acid level in the serum. Additionally,

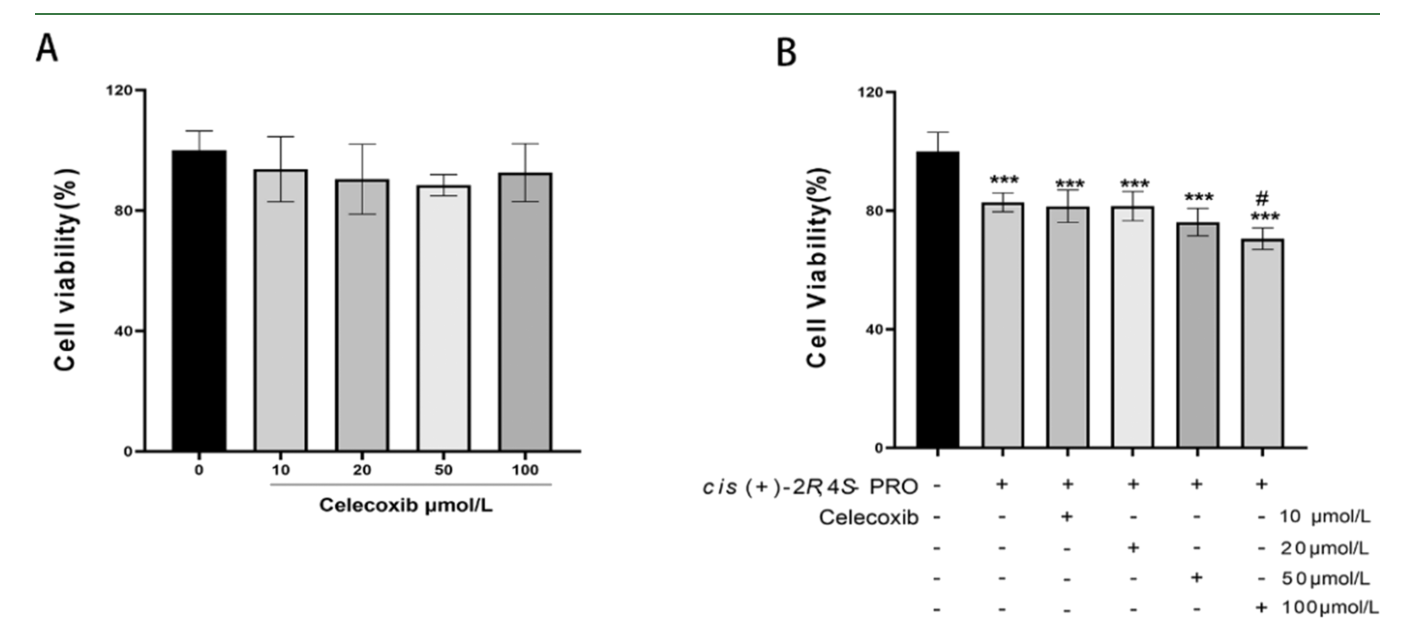


Figure 6. CYP1A2 enzyme inhibitor could exacerbate the cytotoxicity of PRO. (A) The cytotoxic effect of celecoxib on the L02 cell line and (B) synergistic cytotoxic effect of celecoxib and cis(+)-2R,4S-PRO on the L02 cell line. Data are represented as mean \pm SEM of three independent experiments. The significant difference is shown as ***p < 0.001 vs control; *p < 0.05 vs cis(+)-2R,4S-PRO.

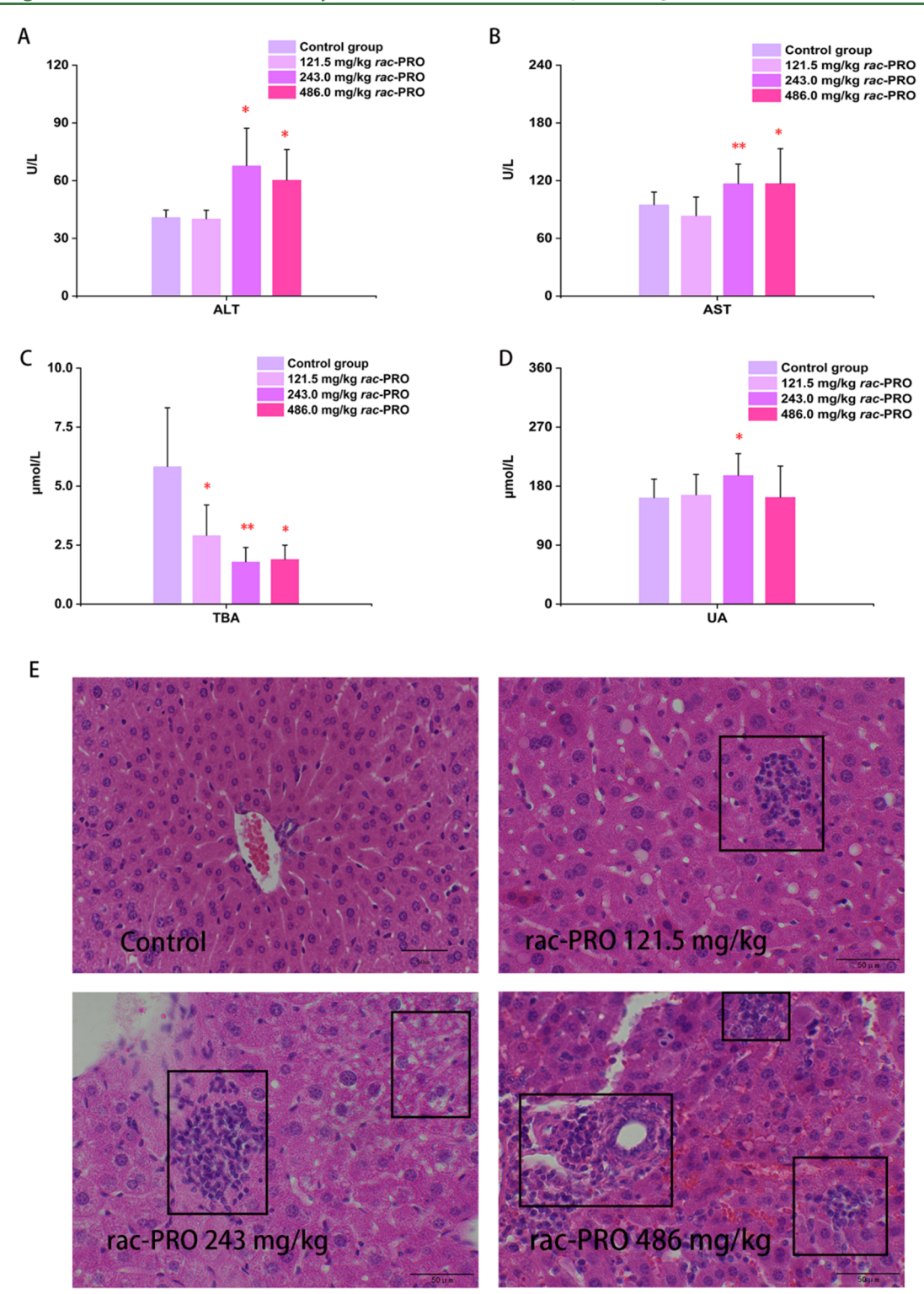


Figure 7. Hepatotoxicity of PRO in mice exposed to *rac*-PRO. PRO significantly affects the liver function of mice, including ALT (A), AST (B), TBA (C), and UA (D). All data are shown as mean \pm SEM, n = 10. The significant difference is shown as *p < 0.05, **p < 0.01 vs control. Representative images showing histological changes in hepatocytes (E).

the hematoxylin—eosin staining results of the liver showed that *rac*-PRO exposure caused pathological changes in the liver, including balloon-like degeneration of liver cells and inflammatory cell infiltration (Figure 7E). All of these results suggested that *rac*-PRO caused hepatotoxicity, and its exposure resulted in liver dysfunction in mice.

3.7. Stereoselective Cytotoxic Effect of PRO on Hepatic Cells. Because our previous study showed that PRO enantiomers exhibited significant stereoselective distribution and metabolic characteristics in the liver, it is necessary to evaluate the stereoselective cytotoxic effects of *rac-PRO* and its stereoisomers on hepatic cells to identify the PRO stereoisomer with the strongest hepatotoxicity. Therefore, we

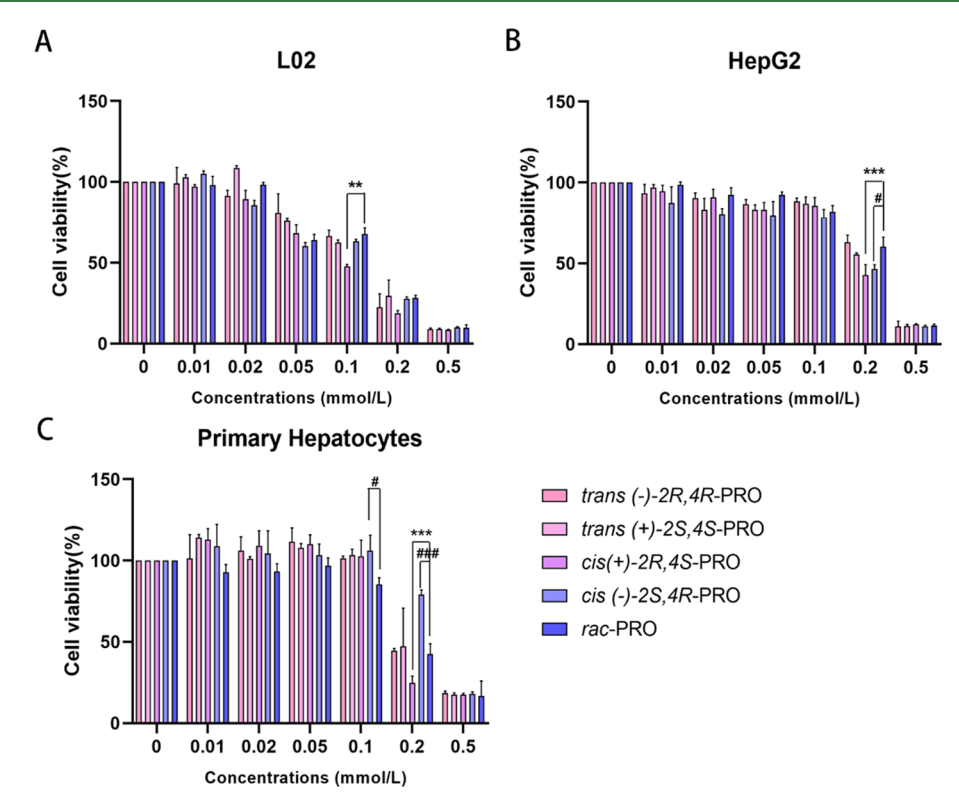


Figure 8. Hepatotoxicity of *rac*-PRO and its enantiomers in (A) the L02 cell line, (B) the HepG2 cell line, and (C) rat primary hepatocytes. Data are represented as mean \pm SEM of three independent experiments. The significant difference is shown as **p < 0.01, ***p < 0.001 *vs rac*-PRO; *p < 0.05, ***p < 0.001 *vs rac*-PRO.

selected hepatic cells to conduct the MTT assay, including the L02 cell line, HepG2 cell line, and rat primary hepatocytes. The exposure concentration range was selected as 0.01-0.5 mmol/L according to our previous study.31 After exposure to rac-PRO and its enantiomers for 72 h, compared with rac-PRO, cis (-)-2S,4R-PRO showed a lower hepatotoxic effect in primary hepatocytes and L02 cell lines. In HepG2 cell lines, the hepatotoxic effect by cis (-)-2S,4R-PRO exposure was lower than that by cis (+)-2R,4S-PRO. The viability of cis (-)-2S,4R-PRO-treated cells was significantly higher than that of other isomers and rac-PRO. However, cis (+)-2R,4S-PRO showed the most significant hepatotoxic effects among the four enantiomers of PRO in the three hepatic cell lines (Figure 8A– C). Since cis (+)-2R,4S-PRO was the isomer that accumulated the most in the liver, our results indicated that the hepatotoxicity of PRO inhalation exposure might be induced by the accumulation of the most hepatotoxic isomer of cis (+)-2R,4S-PRO. In summary, our study not only lays a foundation for developing the single configuration of PRO with a safer ecological balance but also provides inspiration for future scientific research on chiral pesticides.

ASSOCIATED CONTENT

Supporting Information

The Supporting Information is available free of charge at https://pubs.acs.org/doi/10.1021/acs.jafc.4c06923.

Detailed information on the matrix standard curves of PRO enantiomers (PDF)

AUTHOR INFORMATION

Corresponding Authors

Hong Zhang — School of Life science and Biopharmaceutics, Shenyang Pharmaceutical University, Shenyang 110016, China; ⊙ orcid.org/0000-0003-2579-2123; Email: song0688@sina.com

Shiliang Yin — School of Pharmacy, Shenyang Medical College, Shenyang 110034, China; Email: yslal@163.com

Authors

Siman Ma – School of Pharmacy, Shenyang Pharmaceutical University, Shenyang 110016, China

Lanfang Ma – Department of Obstetrics and Gynecology, Guiyang Maternity and Child Health Care Hospital, Guiyang, Guizhou 550003, China

Yanbei Lu — School of Pharmacy, Shenyang Pharmaceutical University, Shenyang 110016, China

Jialin Zhang – School of Life science and Biopharmaceutics, Shenyang Pharmaceutical University, Shenyang 110016, China

Hao Xin – School of Life science and Biopharmaceutics, Shenyang Pharmaceutical University, Shenyang 110016, China

Yuchen Zhou - School of Pharmacy, Shenyang Medical College, Shenyang 110034, China

Shiwen Feng — School of Veterinary and Agriculture Sciences, The University of Melbourne, Melbourne, Victoria 3010, Australia

Ge Jin – School of Pharmacy, Shenyang Medical College, Shenyang 110034, China

Xinyuan Du - Pharmaceutical Research Institute, China Shineway Pharmaceutical Group, Beijing 100025, China Complete contact information is available at: https://pubs.acs.org/10.1021/acs.jafc.4c06923

Funding

This work was financially supported by the National Natural Science Foundation of China (82003971), China Postdoctoral Science Foundation (2021M692227), Basic Research Projects of Liaoning Provincial Department of Education (LJKMZ20221364), Youth Career Development Plan of Shenyang Pharmaceutical University (ZQN202302), and Guizhou Provincial Science and Technology Projects (ZK [2022]YB-004).

Notes

The authors declare no competing financial interest.

ACKNOWLEDGMENTS

The authors wish to thank Professor Xingjie Guo for rendering much assistance in the preparation of this paper.

ABBREVIATIONS

PRO, Propiconazole; RLMs, Rat liver microsomes; MTT, 3-(4,5-Dimethylthiazol-2-yl)-2,5-diphenyltetrazolium bromide; CYPs, Cytochromes P450; L8824 cells, Grass carp liver cells; mRNA, Messenger ribonucleic acid; LC-MS/MS, Chiral liquid chromatography tandem mass spectrometry; IS, Internal standard; MS-grade, Mass spectrum grade; ACN, Acetonitrile; NADPH, β -Nicotinamide adenine dinucleotide phosphate; ATCC, American Type Culture Collection; PBS, Phosphatebuffered saline; L02 cell line, Human embryonic liver cells; HepG2 cell line, Hepatoma cells; FBS, Fetal bovine serum; DMEM, Dulbecco's modified Eagle medium; SD, Sprague-Dawley; KM, Kunming; SPF, Specific pathogen free; EF, Enantiomeric fractions; k, Rate constant of metabolism reaction; $t_{1/2}$, Half-life time (min); V, Metabolism rate; V_{max} Maximum metabolism velocity; S, Substrate concentration; K_{m} , Michaelis constant; CL_{int}, Intrinsic metabolic clearance; LD₅₀, Median lethal dose; H&E staining, Hematoxylin-eosin staining; ALT, Glutamic-pyruvic transaminase; AST, Glutamic oxaloacetic transaminase; UA, Uric acid; TBA, Total bile acid; SEM, Standard error; ANOVA, Analysis of variance; LLOQ, Lower limit of quantitation; R^2 , Correlation coefficients

REFERENCES

- (1) Xu, H.; Zhu, X.; Wang, J.; Lin, Z.; Chen, G. Electro-chemiluminescent functional nucleic acids-based sensors for food analysis. *Luminescence.* **2019**, *34*, 308–315.
- (2) Allen, J. W.; Wolf, D. C.; George, M. H.; Hester, S. D.; Sun, G.; Thai, S. F.; Delker, D. A.; Moore, T.; Jones, C.; Nelson, G.; Roop, B. C.; Leavitt, S.; Winkfield, E.; Ward, W. O.; Nesnow, S. Toxicity profiles in mice treated with hepatotumorigenic and non-hepatotumorigenic triazole conazole fungicides: Propiconazole, triadimefon, and myclobutanil. *Toxicol Pathol.* **2006**, *34*, 853–862.
- (3) Pathan, A. K.; Cuddy, W.; Kimberly, M. O.; Adusei-Fosu, K.; Rolando, C. A.; Park, R. F. Efficacy of Fungicides Applied for Protectant and Curative Activity Against Myrtle Rust. *Plant Dis.* **2020**, *104*, 2123–2129.
- (4) Ware, G. W.1978. The Pesticide Book; Thomson Publications.
- (5) Singh, A.; Dhiman, N.; Kar, A. K.; Singh, D.; Purohit, M. P.; Ghosh, D.; Patnaik, S. Advances in controlled release pesticide formulations: Prospects to safer integrated pest management and sustainable agriculture. *J. Hazard Mater.* **2020**, *385*, No. 121525.
- (6) Jeschke, P. Current status of chirality in agrochemicals. *Pest. Manag. Sci.* **2018**, *74*, 2389–2404.

- (7) Tong, Z.; Dong, X.; Yang, S.; Sun, M.; Gao, T.; Duan, J.; Cao, H. Enantioselective effects of the chiral fungicide tetraconazole in wheat: Fungicidal activity and degradation behavior. *Environ. Pollut.* **2019**, 2019 (247), 1–8.
- (8) Ibrahim, E. A.; Shalaby, S. E. M. Screening and assessing of pesticide residues and their health risks in vegetable field soils from the Eastern Nile Delta. *Egypt. Toxicol Rep.* **2022**, *9*, 1281–1290.
- (9) Jiao, C.; Chen, L.; Sun, C.; Jiang, Y.; Zhai, L.; Liu, H.; Shen, Z. Evaluating national ecological risk of agricultural pesticides from 2004 to 2017 in China. *Environ. Pollut.* **2020**, 259, No. 113778.
- (10) Kieffer, D. A.; Martin, R. J.; Adams, S. H. Impact of Dietary Fibers on Nutrient Management and Detoxification Organs: Gut, Liver, and Kidneys. *Adv. Nutr.* **2016**, *7*, 1111–1121.
- (11) Reed, L.; Arlt, V. M.; Phillips, D. H. The role of cytochrome P450 enzymes in carcinogen activation and detoxication: an in vivo-in vitro paradox. *Carcinogenesis.* **2018**, *39*, 851–859.
- (12) Guengerich, F. P. Cytochrome p450 and chemical toxicology. *Chem. Res. Toxicol.* **2008**, *21*, 70–83.
- (13) Liu, H.; Li, P.; Wang, P.; Liu, D.; Zhou, Z. Toxicity risk assessment of pyriproxyfen and metabolites in the rat liver: A vitro study. *J. Hazard Mater.* **2020**, 389, No. 121835.
- (14) Voican, C. S.; Corruble, E.; Naveau, S.; Perlemuter, G. Antidepressant-induced liver injury: a review for clinicians. *Am. J. Psychiatry.* **2014**, *171*, 404–415.
- (15) Carrão, D. B.; Habenchus, M. D.; de Albuquerque, N. C. P.; da Silva, R. M.; Lopes, N. P.; de Oliveira, A. R. M. In vitro inhibition of human CYP2D6 by the chiral pesticide fipronil and its metabolite fipronil sulfone: Prediction of pesticide-drug interactions. *Toxicol. Lett.* **2019**, *313*, 196–204.
- (16) Guo, D.; He, R.; Su, W.; Zheng, C.; Zhang, W.; Fan, J. Stereochemistry of chiral pesticide uniconazole and enantioselective metabolism in rat liver microsomes. *Pestic. Biochem. Physiol.* **2021**, 179, No. 104964.
- (17) Perovani, I. S.; Santos Barbetta, M. F.; Moreira da Silva, R.; Lopes, N. P.; Moraes de Oliveira, A. R. Moraes de Oliveira, A.R. In vitro-in vivo correlation of the chiral pesticide prothioconazole after interaction with human CYP450 enzymes. *Food Chem. Toxicol.* **2022**, *163*, No. 112947.
- (18) Yan, J.; Zhang, P.; Wang, X.; Xu, M.; Wang, Y.; Zhou, Z.; Zhu, W. Stereoselective Degradation of alpha-Cypermethrin and Its Enantiomers in Rat Liver Microsomes. *Chirality.* **2016**, 28, 58–64.
- (19) Zhao, H.; Wang, Y.; Liu, Y.; Yin, K.; Wang, D.; Li, B.; Yu, H.; Xing, M. ROS-Induced Hepatotoxicity under Cypermethrin: Involvement of the Crosstalk between Nrf2/Keap1 and NF- κ B/i κ B- α Pathways Regulated by Proteasome. *Environ. Sci. Technol.* **2021**, 55, 6171–6183.
- (20) Hu, L.; Xu, T.; Wang, X.; Qian, M.; Jin, Y. Exposure to the fungicide prothioconazole and its metabolite prothioconazole-desthio induced hepatic metabolism disorder and oxidative stress in mice. *Pestic. Biochem. Physiol.* **2023**, *193*, No. 105452.
- (21) Georgopapadakou, N. H. Antifungals: mechanism of action and resistance, established and novel drugs. *Curr. Opin Microbiol.* **1998**, *1*, 547–557.
- (22) Robinson, J. F.; Tonk, E. C.; Verhoef, A.; Piersma, A. H. Triazole induced concentration-related gene signatures in rat whole embryo culture. *Reprod Toxicol.* **2012**, *34*, 275–283.
- (23) VINGGAARD, A.; HASS, U.; DALGAARD, M.; ANDERSEN, H.; BONEFELD–JØRGENSEN, E.; CHRISTIANSEN, S.; LAIER, P.; POULSEN, M. Prochloraz: an imidazole fungicide with multiple mechanisms of action. *Int. J. Androl.* **2006**, *29*, 186–192.
- (24) Zarn, J. A.; Brüschweiler, B. J.; Schlatter, J. R. Azole fungicides affect mammalian steroidogenesis by inhibiting sterol 14 alphademethylase and aromatase. *Environ. Health Perspect.* **2003**, *111*, 255–261.
- (25) Pan, X.; Cheng, Y.; Dong, F.; Liu, N.; Xu, J.; Liu, X.; Wu, X.; Zheng, Y. Stereoselective bioactivity, acute toxicity and dissipation in typical paddy soils of the chiral fungicide propiconazole. *J. Hazard Mater.* **2018**, 359, 194–202.

- (26) Sun, G.; Thai, S. F.; Tully, D. B.; Lambert, G. R.; Goetz, A. K.; Wolf, D. C.; Dix, D. J.; Nesnow, S. Propiconazole-induced cytochrome P450 gene expression and enzymatic activities in rat and mouse liver. *Toxicol. Lett.* **2005**, *155*, 277–287.
- (27) Nesnow, S.; Grindstaff, R. D.; Lambert, G.; Padgett, W. T.; Bruno, M.; Ge, Y.; Chen, P. J.; Wood, C. E.; Murphy, L. Propiconazole increases reactive oxygen species levels in mouse hepatic cells in culture and in mouse liver by a cytochrome P450 enzyme mediated process. *Chem. Biol. Interact.* **2011**, 194, 79–89.
- (28) Bruno, M.; Moore, T.; Nesnow, S.; Ge, Y. Protein carbonyl formation in response to propiconazole-induced oxidative stress. *J. Proteome Res.* **2009**, *8*, 2070–2078.
- (29) Kwon, H. C.; Sohn, H.; Kim, D. H.; Shin, D. M.; Jeong, C. H.; Chang, Y. H.; Yune, J. H.; Kim, Y. J.; Kim, D. W.; Kim, S. H.; Han, S. G. In Vitro and In Vivo Study on the Toxic Effects of Propiconazole Fungicide in the Pathogenesis of Liver Fibrosis. *J. Agric. Food Chem.* **2021**, *69*, 7399–7408.
- (30) Knebel, C.; Kebben, J.; Eberini, I.; Palazzolo, L.; Hammer, H. S.; Süssmuth, R. D.; Heise, T.; Hessel-Pras, S.; Lampen, A.; Braeuning, A.; Marx-Stoelting, P. Propiconazole is an activator of AHR and causes concentration additive effects with an established AHR ligand. *Arch. Toxicol.* **2018**, *92*, 3471–3486.
- (31) Ma, S.; Xin, H.; Zhao, P.; Feng, S.; Chen, J.; Yin, S.; Wei, Y.; Shi, Y.; Jin, G.; Di, X.; Zhang, H. Comprehensive stereoselectivity assessment of toxicokinetics, tissue distribution, cytotoxicity and environmental fate of chiral pesticide propiconazole. *J. Agric. Food Chem.* **2023**, *71*, 19760–19771.
- (32) He, Z.; Wang, Z.; Gao, B.; Liu, S.; Zhao, X.; Shi, H.; Wang, M. Stereostructure-activity mechanism of cyproconazole by cytochrome P450 in rat liver microsomes: A combined experimental and computational study. *J. Hazard Mater.* **2021**, *416*, No. 125764.
- (33) Li, L.; Shi, H.; Hua, X.; Wang, M.; Wang, H. Intrinsic Clearance and Metabolism Pathway of Fosthiazate in Rat and Cock Liver Microsomes: From Chiral Assessment View. *J. Agric. Food Chem.* **2021**, *69*, 12654–12660.
- (34) Li, L.; Xu, J.; Lv, B.; Kaziem, A. E.; Liu, F.; Shi, H.; Wang, M. Chiral Organophosphorous Pesticide Fosthiazate: Absolute Configuration, Stereoselective Bioactivity, Toxicity, and Degradation in Vegetables. J. Agric. Food Chem. 2020, 8, 7609–7616.
- (35) Lin, C.; Miao, Y.; Qian, M.; Wang, Q.; Zhang, H. Enantioselective Metabolism of Flufiprole in Rat and Human Liver Microsomes. J. Agric. Food Chem. 2016, 64, 2371–2376.
- (36) Liu, N.; Dong, F.; Xu, J.; Liu, X.; Zheng, Y. Chiral bioaccumulation behavior of tebuconazole in the zebrafish (Danio rerio). *Ecotoxicol. Environ. Saf.* **2016**, *126*, 78–84.
- (37) Gao, B.; Zhao, S.; Zhang, Z.; Li, L.; Hu, K.; Kaziem, A. E.; He, Z.; Hua, X.; Shi, H.; Wang, M. A potential biomarker of isofenphosmethyl in humans: A chiral view. *Environ. Int.* **2019**, *127*, 694–703.
- (38) Zhang, Q.; Ji, S.; Chai, L.; Yang, F.; Zhao, M.; Liu, W.; Schüürmann, G.; Ji, L. Metabolic mechanism of arylphosphorus flame retardants by cytochromes P450: a combined experimental and computational study on triphenyl phosphate. *Environ. Sci. Technol.* **2018**, *52*, 14411–14421.
- (39) Lu, L.; Zhan, T.; Ma, M.; Xu, C.; Wang, J.; Zhang, C.; Liu, W.; Zhuang, S. Thyroid disruption by bisphenol S analogues via thyroid hormone receptor β : in vitro, in vivo, and molecular dynamics simulation study. *Environ. Sci. Technol.* **2018**, *52*, 6617–6625.
- (40) Karjalainen, M. J.; Neuvonen, P. J.; Backman, J. T. Celecoxib is a CYP1A2 inhibitor in vitro but not in vivo. *Eur. J. Clin. Pharmacol.* **2008**, *64*, 511–519.